The effect of rock type on natural water flooding and residual oil saturation below free water level and oil water contact: A case study from the Middle East

E. Heydari-Farsani[1,*]; J. E. Neilson[1]; G.I. Alsop[1]; H. Hamidi[2]

1) **School of Geosciences, King's College, University of Aberdeen, Aberdeen, AB24 3UE, UK**
2) **School of Engineering, King's College, University of Aberdeen, Aberdeen AB24 3UE, UK**

Abstract

The presence of residual oil below the present day free water level (FWL) and oil water contact (OWC) is common in many fields of the Middle East. This residual oil is seen in reservoirs prior to the start of production.

A rock typing study was carried out to investigate the effect of rock types on the presence and distribution of residual oil below the free water level (FWL) and oil water contact (OWC) and potential recovery from ROZ's following water flooding.

The rock typing study was carried out by integration of different data sources i.e. core description, thin section study, conventional core analysis (CCAL), special core analysis (SCAL) and petrophysical logs. Six major rock types with unique reservoir quality and behaviour were classified in cored wells and subsequently predicted in un-cored wells. Reservoir quality increases from rock type 1 to 6.

The residual oil saturation (Sor) of each rock type was defined and it was concluded that all rock types except for rock type 1 contain residual oil below the present day FWL and OWC. The absence of residual oil in rock type 1 was related to the fact that it is unlikely that oil migration into it ever occurred and consequently no residual oil is seen below the present day FWL and OWC. It was also revealed that rock type 6, with better porosity and permeability,

includes the highest residual oil saturation. This was attributed to its bimodal pore throat size distribution and the effect of this on water flooding and hence potential recovery.

Keywords: Rock typing, Residual oil, Sarvak Formation, Mishrif, Carbonate reservoir, Middle East, Offshore Iran.

1. Introduction

The studied field (Field A), which is located in the south-east of the Persian Gulf in the Middle East (Figure 1), presents a residual oil zone (ROZ) below the FWL and OWC (Figure 2). This ROZ below the FWL and OWC existed prior to the start of production. Characterization of reservoirs with a ROZ below the FWL and OWC prior to the start of production is challenging as they show abnormal behaviour e.g. dry oil production close to FWL. Also, significant reserves of oil can occur below the FWL and OWC if ways to produce them could be found, but the first step is to better understand their origin and distribution. Therefore, the goal of this study is to investigate the role of rock type on the distribution of residual oil below the FWL and OWC in the carbonate reservoir of Field A.

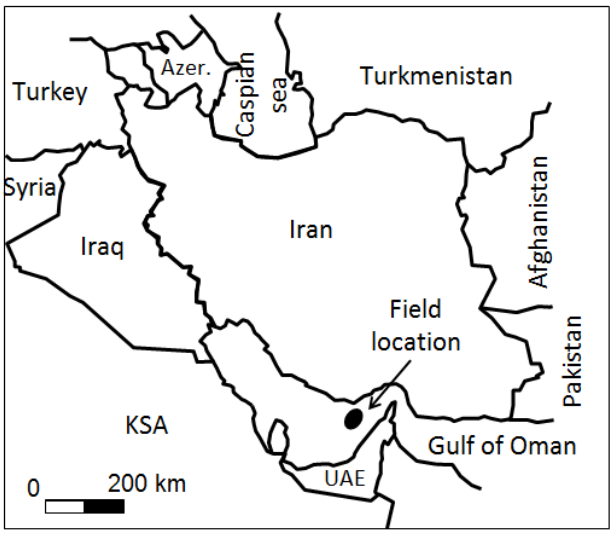

Figure 1: Location of the Field A in the Persian Gulf.

Field A presents a FWL obtained from the formation pressure data in a northern well (A6). This FWL is supported by the same OWC depth determined from the log data in two southern and one northern well. A ROZ occurs below the FWL and OWC in the northern parts of the field (Figure 2).

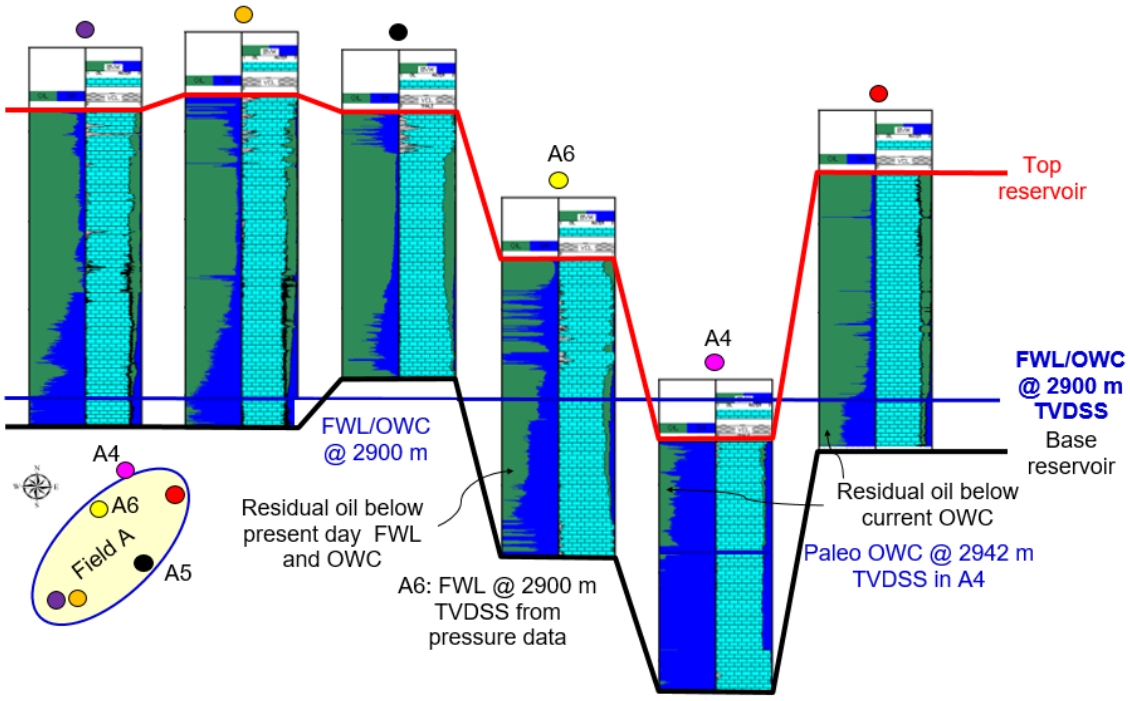

Figure 2: Presence of residual oil below FWL and OWC in the studied field.

Reservoir rock typing is a key technique in modern reservoir studies and is the practice by which geological facies are categorised by their petrophysical properties.

Archie (1950) first defined a rock type as units of rock deposited under similar conditions and which experienced similar diagenetic processes, resulting in a unique porosity-permeability relationship, capillary pressure profile and water saturation for a given height above the free water level in a reservoir. Rock typing was subsequently described in several papers (e.g. Davies et al., 1991; Porras, et al., 1999; Porras and Campus, 2001; Boada, 2001; Soto, 2001; Marquez et al., 2001; Lee, et al., 2002; Al-Habshi et al., 2003; Ali-Nandal and Gunter, 2003;

Perez et al., 2003; Al-Farisi et al., 2004; Ohen et al., 2004; Shenawi et al., 2007, Slatt, 2007, Nouri-Taleghani et al., 2015 and Ghadami et al., 2015). Various geological (depositional environment, texture, grain size and sorting), petrophysical (porosity, permeability, flow zone indicator and water saturation) and reservoir (pore throat size, capillary pressure curves and wettability) data have been used in these studies to define rock types. One of the most important conclusions reported by authors is rock typing is very challenging subject in carbonate reservoirs, due to their typical heterogeneity, diagenesis, rock/fluid interaction and scale issues and requires maximum data integration. In this study therefore rock types were classified by data integration.

Studies on residual oil have mostly focused on the remaining and residual oil in the transition zone. Kirkham et al. (1996) studied fluid saturation prediction in the transition zone of fields with residual oil in the United Arab Emirates (UAE). Mezler et al., (2006) and Koperna et al., (2006) reported significant oil reserves in the residual oil zones (ROZs) of the Permian Basin, USA. The production characteristics of ROZs have been reported on by Parker and Rudd (2000, Middle East reservoirs), Koperna et al., (2006, USA) and Harouaka et al., (2013; Permian Basin reservoirs, USA). Pelissier et. al., (1980) studied the hydrodynamic activity in some of the Middle East reservoirs and its effect on ROZ's. Thomasen and Jacobsen, (1994) and Vejbaek et al., (2005) evaluated the relationship between active hydrodynamic drive and the presence of ROZs in the North Sea reservoirs, and Aleidan at al., (2017) carried out a palaeo-oil characterisation and fundamental analysis of the ROZ for a field in Saudi Arabia. Heydari-Farsani et al., (2019) attributed the presence of residual oil below the fluid contact in the Persian Gulf to the Zagros orogeny and flexural loading in the Persian Gulf foreland basin.

No study has been found that investigates the relationship between rock types and residual oil below the FWL and OWC in the Persian Gulf area and it is anticipated that the results of this

study will appeal to many readers in the area of petroleum geology and reservoir characterisation given novel nature of the work.

2. Geological setting and field description

The studied field forms an elongated NNE–SSW anticlinal structure, situated 80 km off Iran's mainland coast in the southern Persian Gulf, close to Gheshm Island. It is located in what was the eastern part of an intrashelf basin within the Arabian continental shelf (Figure 3) that developed during the middle Cretaceous (Jordan et al., 1985; Alsharhan and Nairn, 1997; Ziegler, 2001). Within this intrashelf basin, the Khatiyah Formation (Fm.) facies (end of the Early Cretaceous) was deposited under anoxic conditions, with the preserved organic matter turning the Khatiyah Fm. facies into a source rock. This intrashelf basin is surrounded by concentric shelf facies belts, including fore-shoal, shoal, back shoal and protected platform facies, corresponding to the late Cretaceous Cenomanian–Turonian Sarvak (Mishrif) Fm., which forms the reservoir. The overall progradation of these facies has created a petroleum system in which the carbonate reservoirs of the Sarvak (Mishrif) Fm. overlie the source rocks of the Khatiyah Fm. (Farzadi, 2006). The seal to the Sarvak (Mishrif) reservoir is provided by 2–5 m of overlying late Cretaceous Coniacian Laffan Fm. shale (Farzadi, 2006).

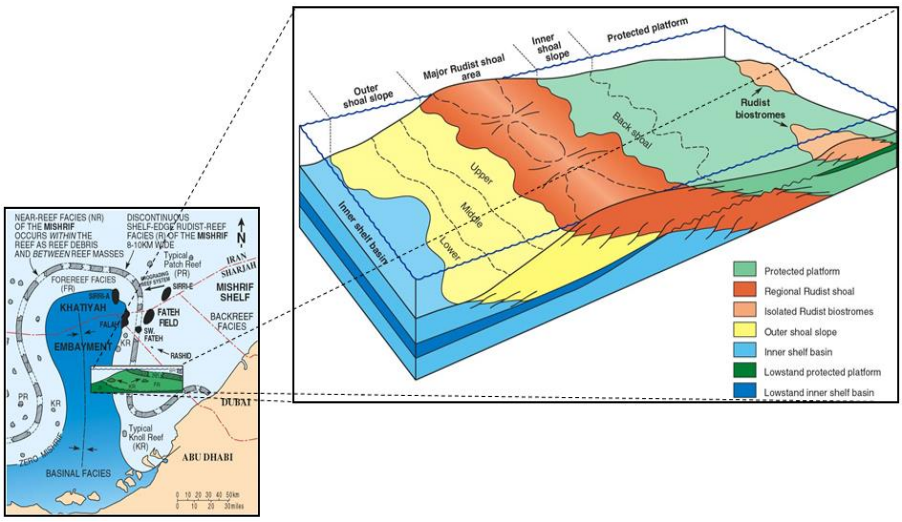

Figure 3: Regional geological depositional setting of the studied field. The overall progradation of facies has generated a petroleum system (after Jordan et al., 1985).

3. Methodology

Petrophysical evaluation was carried out using all available logs, core data (CCAL and SCAL), formation pressure data (RFT in this field), drill stem test (DST) and mud logging gas data for each of the wells. Shale volume, porosity (effective and total), water saturation (effective and total), movable and residual oil saturation and net intervals were calculated from quality checked logs.

The FWL, OWC, oil down to (ODT) and water up to (WUT) were defined for all wells using the results of petrophysical evaluation, pressure and test data, core oil staining and mud logging gas data.

The FWL is the point at which the water saturation is 100% and capillary pressure (pressure of the non-wetting phase - pressure of the wetting-phase) is zero (Spinler and Baldwin, 1999; Darling, 2005; Tiab and Donaldson, 2015). It is best defined using pressure data and in practice it is a hydraulic surface marking the intersection between the hydrocarbon zone gradient and water zone gradient on a formation pressure vs. depth cross plot.

The OWC is the level at which the hydrocarbon saturation starts to increase from some minimum. At the OWC, capillary pressure is not zero (Elshahawi et al., 1999). The OWC is best defined using logs, core, test and mud logging gas data.

For the purpose of rock typing, three cored wells (A5, A6 and A38) located in the north, south and east of the field were selected as key wells and their data analysed.

Major rock types were identified by integration of CCAL, SCAL, sedimentlogical studies and logs in cored wells (Figure 4). In addition to the results of core description and thin section

study, the relationship between porosity and permeability was investigated using the Amaefule method (Amaefule et al, 1993). The Flow Zone Indicator (FZI) of each CCAL sample was calculated using core porosity and permeability. Although successful application of the FZI method in carbonate rock typing has been reported in many studies (e.g. Ghadami et al., 2015, Aliakbardoust and Rahimpour, 2013 and Chandra et al., 2015), it was used in this study in combination with other data and not in isolation. Pore throat size distribution (diameter) calculated from available MICP data was directly used in the rock typing study after quality checking. Classified rock types were predicted in uncored wells using log responses for each rock type.

Residual oil below the fluid contact of each rock type was calculated from petrophysical results and whole core water flooding study and possible relationship between the rock types and the presence of the residual oil below the FWL and OWC was investigated.

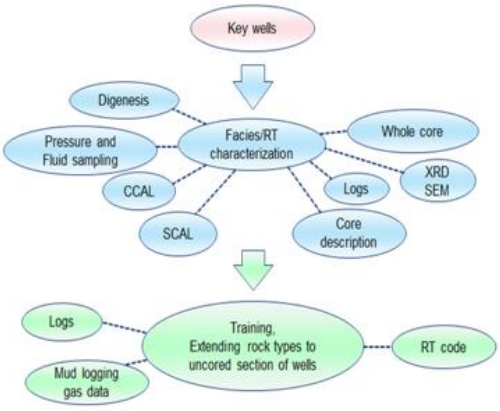

Figure 4: Rock typing methodology and data

4. Available data

Rock typing in carbonate reservoirs is very complex and challenging (Ghadami et al., 2015). They present a high level of heterogeneity and require multi-scale data to characterize them (Alabi et al., 2014 and Chitale et al., 2015). In the meantime, in many exploration and

development projects, including this field, financial considerations limit data gathering. To achieve maximum information from the available budget in this field, the operator only gathered conventional data (e.g. traditional wireline logs, core data, formation pressure test and drill stem test).

4.1. Core description

Wells A5, A6 and A38 yielded 252 m of core description (A5: 92 m, A6: 86.5 m and A38: 73.5 m). Cores were cut using a water-based mud with very good recovery factors. Visual porosity and permeability, oil staining, diagenesis and texture (Dunham, 1962) were studied and used for rock typing. Cores provided detailed interpretations of the sedimentary character and development of the complete Sarvak (Mishrif) Fm.

In the uppermost part of the Sarvak (Mishrif) Fm., sediments are generally composed of bedded benthonic foraminiferal (abundant miliolids) and peloidal mudstone and wackestone (Figure 5 A), rich in mollusc and green algal debris. These facies are sometimes argillaceous, interrupted by frequent hardgrounds or firmgrounds that represent sedimentation breaks and possible subaerial exposure. They are often extensively burrowed and mottled, producing a characteristic nodular fabric.

The Upper Sarvak (Mishrif) presents a complex sedimentology. All cored wells display coarse-grained shelly bioclastic grainstone. Interskeletal matrices are composed of finer molluscan packstone or wackstone rich in benthic forams and green algal debris. The sediments are more varied, stylolitized and indurated than other coarse facies in the Upper Sarvak (Mishrif) (Figure 5 B). Bioturbation is extensive and only occasional cross bedding is preserved. These sediments represent a shoal environment.

The Lower Sarvak (Mishrif) Fm. (Figure 5 C) is composed of a thick and homogeneous bioclastic sedimentary package that records the progradation of the Sarvak (Mishrif) platform within the Khatiyah Basin. Progradation is shown by a general coarsening upward sequence. Stylolitization also decreases upward as the proportion of coarser bioclastic material increases and finer fractions decrease (e.g. clays/organic matter). At the base, facies are generally represented by moderately well-bedded, well sorted, fine-grained bioturbated peloidal wackestone to packstone. At the top of the lower Sarvak (Mishrif), facies are well sorted, medium to coarse-grained peloidal packstones or grainstones, rich in rudist debris and sometimes cross bedded. This progradational succession indicates shallow open marine depositional environments located on the slope in front of the shoal. The absence of re-sedimented material or slumps indicates that the slope had a very low gradient.

The transition between the Khatiyah and Sarvak (Mishrif) Formations is clearly exposed in cores. The uppermost part of the Khatiyah Formation and lowest part of the Sarvak (Mishrif) Formation consist of dark shaley mudstones (Figure 5 D) and burrowed argillaceous limestones. Bioclasts are rare, and mainly composed of very small grained peloids, bivalve debris and numerous planktonic forams. They were deposited in relatively deep water shelf environments. Black, organic-rich intervals suggest that the environment was periodically restricted.

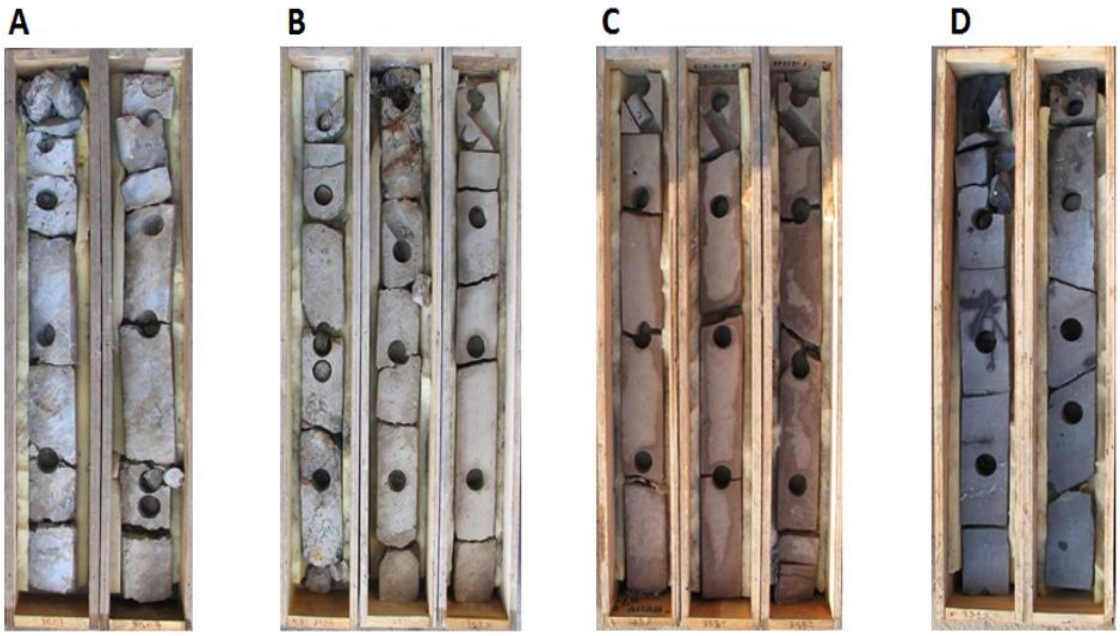

Figure 5: Main lithofacies of the Sarvak (Mishrif) Formation. A: Top of the Sarvak is mainly composed of mudstone and wackestone, B: Upper Sarvak (Mishrif) mainly comprises coarse-grained shelly bioclastic grainstone, C: Lower Sarvak (Mishrif) is mainly composed of wackestone to packstone, D: Transition between Khatiyah and Sarvak (Mishrif) consist of dark shaly mudstones

4.2. Thin section study

Thin section study reports of wells A5, A6 and A38 (392 thin-sections for A5, 380 for A6 and 165 for A38) were used in this study. The presence and the amount of porosity and permeability, microfacies, diagenetic effects and texture (Dunham, 1962) were used for rock typing.

4.3. Conventional core analysis (CCAL)

A total of 937 core plug samples and related CCAL data from three wells (A5: 392, A6: 380 and A38: 165) were available for this study (Figure 6). Core porosity and permeability data were used for rock typing after a quality check, stress correction, the removal of outliers (a few

samples with high permeability reported as samples with induced fracturing) and depth shifting (correcting depth of core data by matching against logs).

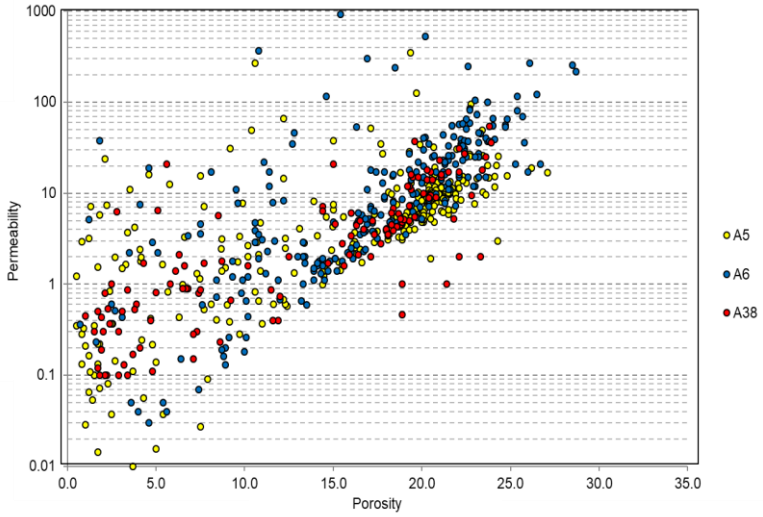

Figure 6: Porosity-permeability cross plot of A5, A6 and A38 wells

4.4. Special core analysis (SCAL)

A total number of 83 mercury injection capillary pressure (MICP) tests (A5: 46 and A6: 37) from special core analysis data were available for this study. The samples analysed cover a wide range of reservoir quality and lithofacies.

In addition to capillary pressure data, the results of two water flood experiments on composite cores were implemented to assess water flooding efficiency in two different rock types. These tests were carried out under reservoir conditions (4680 psi and 109 °C) using oil and water similar to the actual reservoir fluids. The required plugs for this test were cut perpendicular to the axis of core (horizontal) and cleaned using a Soxhlet extractor unit. They were scanned using Computed Tomography (CT) to make sure they were homogeneous and representative of one rock type. Plugs were set separately into a Hassler cell at ambient conditions with a confining pressure and air permeability was measured. Toluene injection followed by water

injection led to measure rock porosity for each sample. Water permeability was also measured at this stage with each plug fully water saturated. A centrifugation device was used to reduce the water saturation from 100% to an expected saturation from the electrical log.

For rock type 6, four plugs were merged and coated in one composite core. For rock type 4, two plugs were merged in one composite core. Once built composite cores were separately set into a Hassler cell at reservoir conditions. Finally, reservoir oil was injected to displace the tank oil and to homogenize the water saturation profile. After reservoir oil breakthrough at the outlet of the composite core sample, oil injection continued until the gas-oil ratio and the oil density at the outlet of the experimental cell reached the values corresponding to the reservoir oil characteristics. Each core with reservoir oil was then aged for one week to restore reservoir wettability. Permeability to reservoir oil at Swi was measured at this stage.

4.5. Petrophysical logs

Petrophysical logs were used in both petrophysical evaluation and rock typing. A large set of wireline and logging while drilling (LWD) logs was available. Gamma ray, neutron porosity, density, shallow and deep resistivity were most commonly used in the study. There is no Nuclear Magnetic Resonance (NMR) data for this field. All available logs were visually inspected using cross plots and layouts. Sections of bad-hole were identified using the caliper (where an over-sized bore hole is shown by the difference between the caliper and the bit size) and density correction log (DRHO). A few wells contained intervals of poor electrical logs due to borehole washouts and other problems.

5. Results

5.1. Petrophysical evaluation and fluid contact (FWL and OWC) determination

Shale volume, porosity, water and hydrocarbon saturations were calculated from quality checked logs.

The FWL, OWC, oil down to (ODT) and water up to (WUT) were defined for all wells in the studied field. This field has a FWL at 2900 m TVDSS, obtained from the formation pressure data (Figure 7). There are also three preproduction wells (A30, A38 and A39) located in the north and south of the field that display OWCs (determined mainly from log data) with almost similar depths (Figure 2).

Based on the petrophysical interpretation and fluid contact determination performed, the present day FWL and OWC in this field does not correspond to 100% Sw but 50% to 60% Sw in some areas of the field. This indicates that there is a residual oil zone (ROZ) below the present day FWL and OWC (Heydari-Farsani et al., 2019).

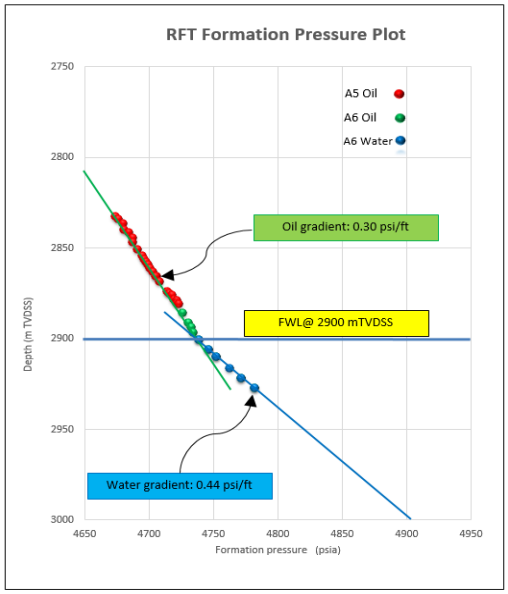

Figure 7: Cross plots of formation pressure data vs depth (TVDSS) shows a FWL at 2900 m TVDSS in studied field.

A typical example of the presence of residual oil below FWL is given by the well A6. This appraisal well was drilled to locate the oil/water contact in the northern part of the field, determine the thickness of the reservoir and asses the characteristics and the productivity of the reservoir. A6 has petrophysical logs, mud logging gas data, core data, formation pressure data (RFT) and drill stem test (DST) data. Analysis of formation pressure data leads to a clear FWL at 2900 m TVDSS (Figure 7 and Track 9 in Figure 8). However, the results of the petrophysical evaluation indicate a significant percentage of residual oil below this depth (Track 9 in Figure 8) where residual oil saturation (Sor) is computed to be around 50% below 2900 m TVDSS. Also, medium brown oil stained core is present below the FWL (Track 10 in Figure 8).

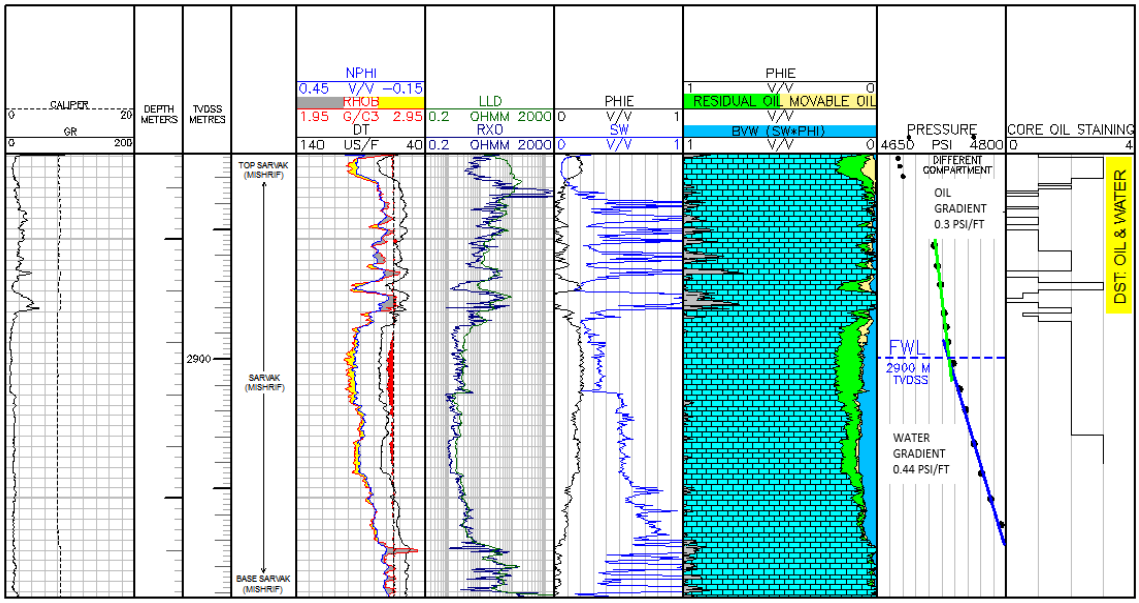

Figure 8: Petrophysical evaluation of A6 showing a FWL at 2900 TVDSS. There is a thickness of residual oil zone and oil staining below this FWL.

5.2. Rock typing

Six major rock types were identified in two key wells (A5, A6). As mentioned earlier they were classified based on their depositional environment, texture, pore type, pore throat size, porosity, permeability and FZI. Table 1 and Figure 9 show details of each rock type.

Significant efforts were made to ensure that the following criteria were met in accordance with the requirements of Varavur et al., (2005) for rock typing studies.

- Each rock type presents a unique reservoir behavior
- Rock types are predictable with satisfactory accuracy using logs in un-cored wells
- 3D distribution of the rock types is predictable within the geological framework

Sedimentary textures (Dunham, 1962), structures, and grain type were studied and used to identify the depositional environments and sub environments. Four main lithofacies of protected platform, shoal, upper slope and lower slope were identified. As it is not recommended to merge different lithofacies at this stage (Gomes et al., 2008), both upper and lower slope lithofacies types were preserved. In the next phase, and to investigate the reservoir behavior of each lithofacies type, the rock fabric, diagenetic processes and particularly pore throat specification were added to the study by applying CCAL, SCAL and FZI data. This new integration shows that sediments of the protected platform, lower and upper slope present a distinct reservoir behaviour, and no further subdivisions are required. They were named rock types 1, 2 and 3 accordingly. However, as it is shown in Table 1, Figures 9 and 10, the shoal lithofacies displays a significant variation in cementation, pore throat size and FZI, and can therefore be divided into three rock types of 4, 5 and 6. Cementation decreases from rock type 4 to 6 while permeability, pore throat size and FZI increase from rock type 4 to 6.

Table 1: Main classified rock types in cored wells and their details.

Rock Type	Depositional environment	Texture	Pore type	Pore throat size	Average porosity %	Average permeability mD	FZI
RT 1	Protected platform	Tight wackestone	Primary	Micro pore	4	<1	FZI<0.45
RT 2	Upper slope	wackestone and packstone	Primary and minor secondary	Micro pore	11	2.5	0.45<FZI<0.56
RT 3	Lower slope	Packstone	Primary and secondary	Meso pore	19	6.5	0.56<FZI<0.9
RT 4	Shoal	Slightly cemented grainstone	Primary and secondary	Macro pore	22	26	0.9<FZI<1.38
RT 5	Shoal	Slightly cemented coarse grainstone	Primary and secondary	Macro pore	23	35	1.38<FZI<1.65
RT 6	Shoal	Coarse grainstone	Primary and secondary	Macro pore	23	45	1.65<FZI

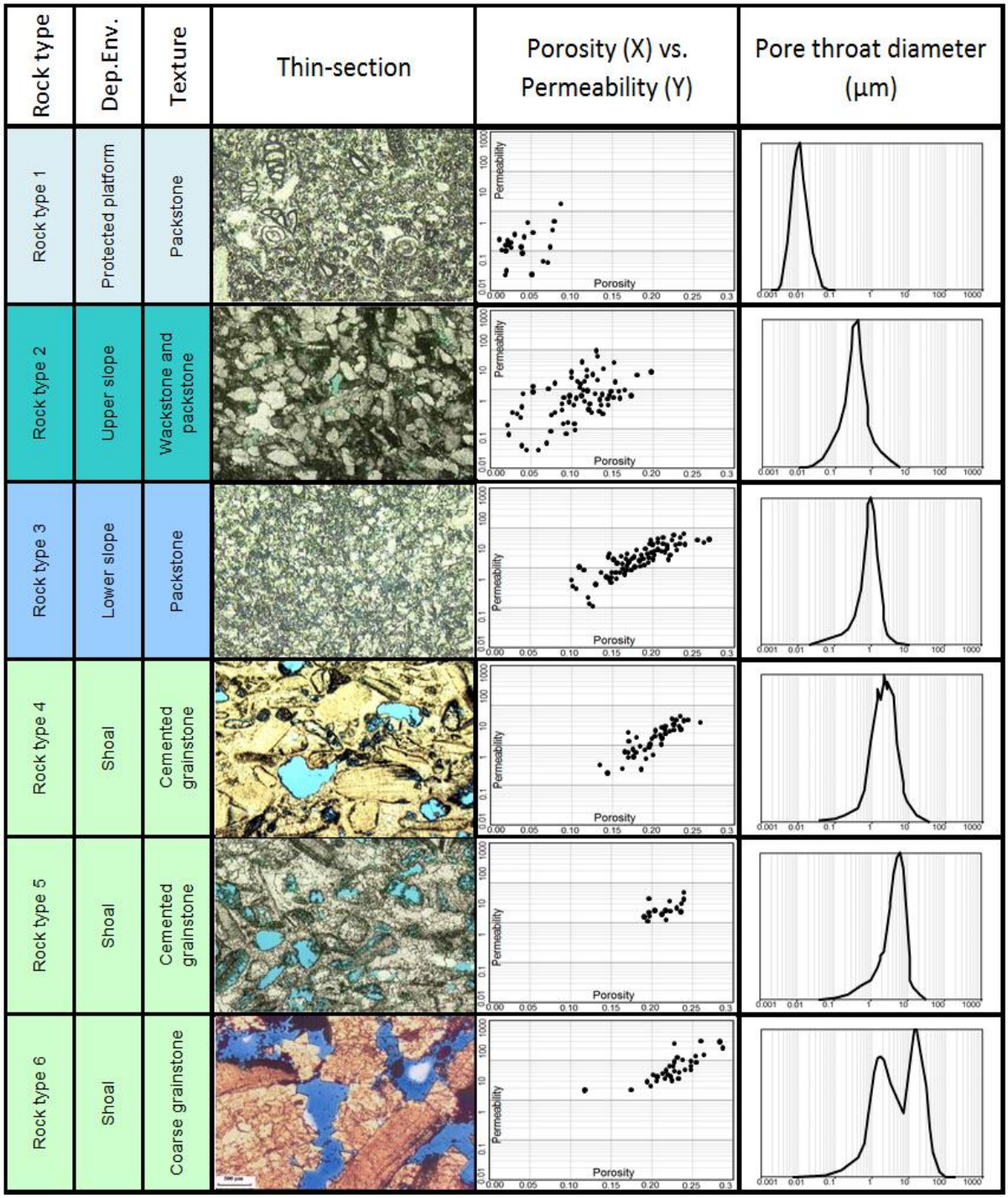

Figure 9: Six major rock types classified by data integration.

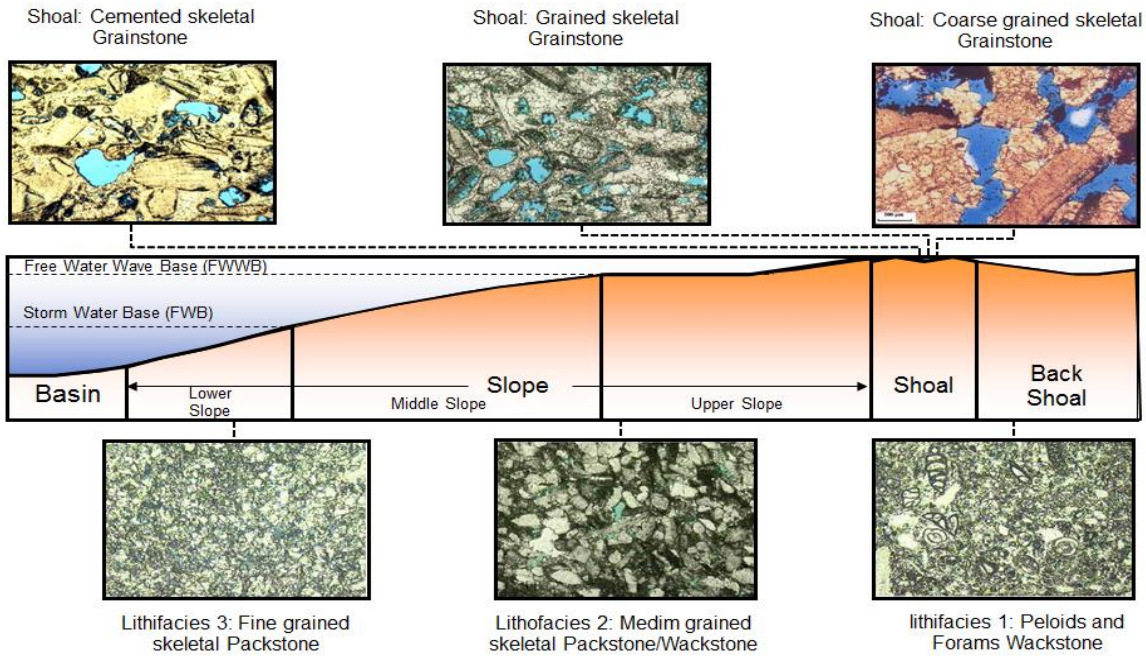

Figure 10: Six major rock types and their depositional environment

Rock type 1: Rock type 1 is preserved in the protected platform and mainly comprises wackstone with peloids and frequent forams. Matrix porosity is very low and dissolution is absent. This rock type has a very low porosity (less than 0.1 v/v) and permeability (less than 1 mD). Pore throat diameter ranges from 0.01 to 0.1µm and pores are classified as mirco pores (Hartmann and Beaumont, 2000) which are consistent with a low FZI value of <0.45.

Rock type 2: Rock type 2 is preserved within the upper slope. It is composed of wackstone and packstone with benthic forams. Data are slightly scattered on the porosity-permeability cross plot. Average porosity is 10 % while permeability varies from 0.1 mD to more than 10 mD. Average pore throat diameter is 0.3 µm which is greater than in rock type 1 (ranges from 0.04 to 3µm). Pores are classified as mirco pores (Hartmann and Beaumont, 2000). FZI is greater than 0.45 and less than 0.56.

Rock type 3: Rock type 3 is the main rock type of the lower slope and is largely composed of packstone. Both matrix porosity and dissolution are present. This rock type presents medium

to high porosity (15 to 25 %) and low to medium permeability (1 to 20 mD). Average pore throat size is 1 µm and varies from 0.07 to 5 µm. This size of pore throat diameter is large enough to create meso pores (Hartmann and Beaumont, 2000). FZI is greater than 0.56 and less than 0.9.

Rock type 4: Rock type 4 is preserved within the shoal environment and is composed of grainstone and coarse grained packstone. Bivalves, rudists and cortoids are common in thin sections of this rock type. Mouldic and vuggy porosity are seen but primary porosity is very low because of cementation. Porosity and permeability show very good correlation. Porosity is more than 15 % and less than 25 % and permeability is between 4 to 50 mD. Pore throat size is between 0.1 to 12 µm (with an average diameter of 3 µm) which results in macro pores in this rock type (Hartmann and Beaumont, 2000). The FZI is greater than 0.9 and less than 1.38.

Rock type 5: Rock type 5 is very similar to rock type 4 but shows slightly better reservoir quality. Rock type 5 is seen within the shoal environment and is composed of coarse grainstone and packstone with abundant bivalves and rudists. Larger mouldic and vuggy porosity occurs but primary porosity is absent because of cementation. Both porosity and permeability show very limited variation. Average porosity is 0.25 v/v and average permeability is 20 mD. Pore throat size varies from 0.1 to 12 µm, and average pore throat size is around 5 µm, which is greater than that in rock type 4. Pores of this rock type are classified as macro pores (Hartmann and Beaumont, 2000). The FZI is between 1.38 and 1.65.

Rock type 6: Rock type 6 is preserved within the shoal environment and is a coarse grainstone with rudist debris and bivalves. Both porosity and permeability are highest in this rock type. Porosity ranges from 20 to 30 % v/v and permeability varies from 20 mD to more than 100 mD. Pore throat diameter is greater than 0.07 µm and, except for a few samples, less than 100 µm. This rock type presents a bimodal pore throat size distribution. The first mode, which

shows a pore throat diameter of 2 µm, represents primary porosity, while a second mode with a value of 11 µm displays very well connected vuggy porosity (Figure 9). In general, pores are macropores (Hartmann and Beaumont, 2000). Well-developed permeability results in a high FZI of greater than 1.65 for this rock type.

The capillary pressure curves of classified rock types are shown in Figure 11.

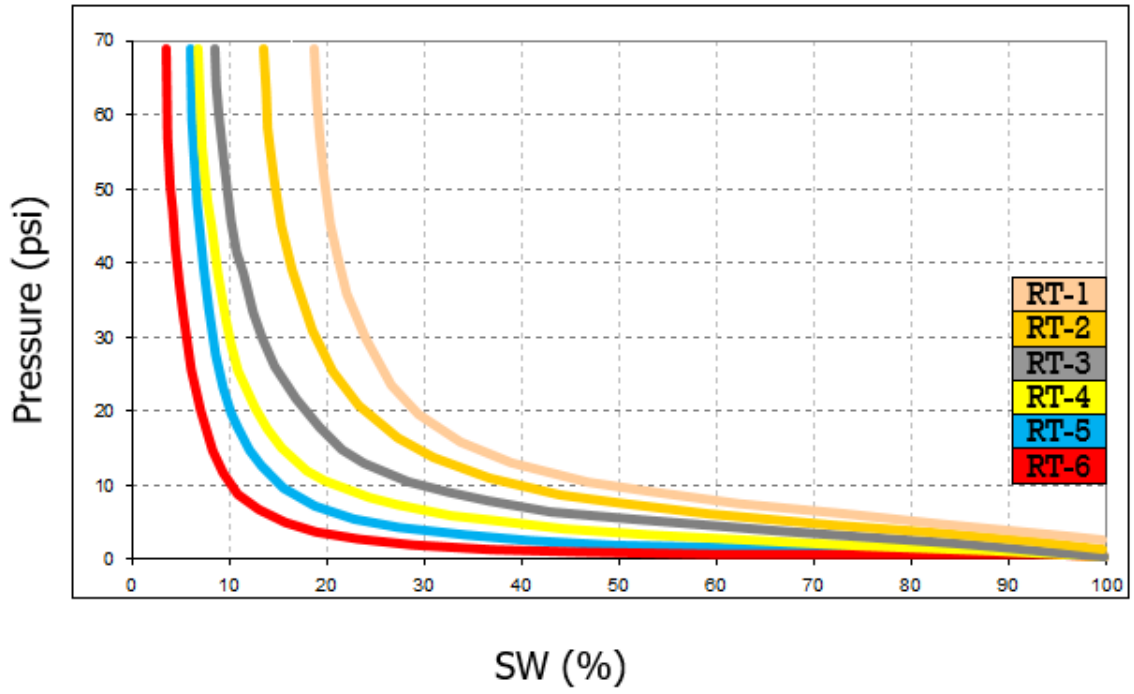

Figure 11: Capillary pressure curves of classified rock types

Rock types were predicted in A38 (a cored well that was used for a blind test and to validate prediction results) and un-cored wells by means of statistical analysis and log responses for each rock type. The ranges of different logs and their ratio for each specific rock type were identified in wells A5 and A6 and each rock type was characterized by a range of values from different logs. In general, GR and RHOB decrease from rock type 1 to 6, while NPHI and DT increase from rock type 1 to 6. Also, many log cross plots were prepared to determine the location of each rock type on the cross plots.

Figure 12 shows a comparison between core rock types (track 7) and predicted rock types (track 8). The results show a very good match between the rock types identified in core and the predicted rock types.

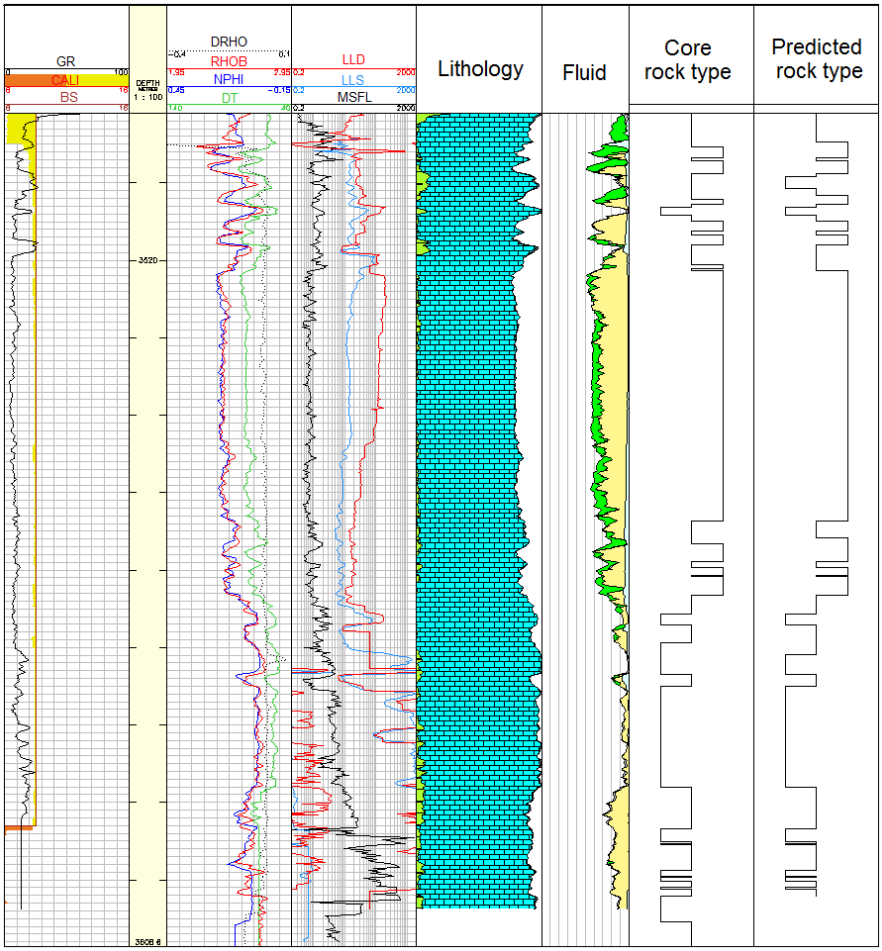

Figure 12: Rock type prediction in A38 shows a very good match between core (track 7) and predicted rock types (track 8)

5.3. Relationship between presence of residual oil and rock types

Residual oil saturation (calculated in petrophysical evaluation) of each rock type was calculated from the FWL and OWC to the base of the Sarvak (Mishrif) Fm and the relationship between the presence and saturation of the residual oil and rock type was investigated for the intervals located below the FWL and OWC. Figure 13 shows an example of this study in well A 6. The

second track shows lithology, porosity, moveable and residual oil saturation and bulk volume of water. The rock type code is seen in the third track.

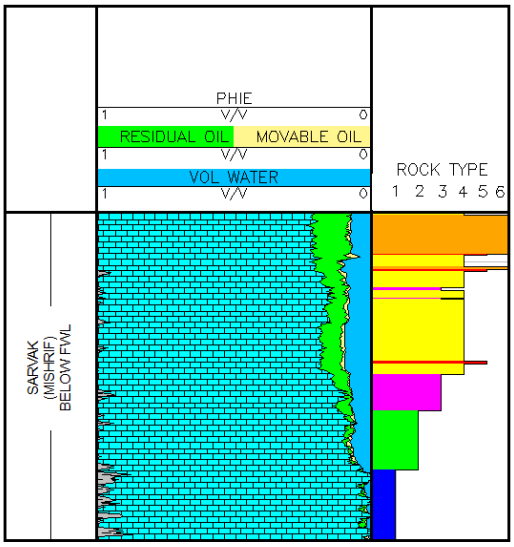

Figure 13: Petrophysical evaluation of A 6 from FWL to the base of the Sarvak (Mishrif) Fm.

6. Discussion on the effect of rock types on distribution and saturation of residual oil below FWL and OWC

Prior to the start of reservoir production, residual oil below the FWL and OWC generally occurs because of the natural and geological water flooding of an oil reservoir (O'Sullivan et al., 2010; Aliedan et al., 2016). The main processes that generate ROZs below fluid contacts are (Melzer et al., 2006):

- Breaching and reforming of the seal;
- An altered hydrodynamic flow field; and
- Regional or local basin tilt.

The ROZ below the fluid contact in this field was generated by regional tectonic tilting and oil remobilization (Heydari-Farsani et al., 2019). Residual oil was left behind because oil was displaced by the spontaneous imbibition of formation waters into the reservoir as the oil

evacuates upwards after a downward tilting of the entire Persian Gulf foreland basin (Heydari-Farsani et al., 2019).

Generally, residual oil is seen when water displaces the oil and leaves residual droplets behind within the pore space. The residual oil saturation and its distribution depend on a number of factors. It is mainly contingent on the wettability but water saturation and reservoir quality can also play a role.

Wettability plays important role in residual oil saturation. Water wet reservoirs display maximum residual oil saturation (McPhee et al. 2015). In these group of reservoirs, grains are covered by a thin film of water and, during the water flooding process where the reservoir quality is similar, oil quickly becomes discontinuous and loses its mobility (McPhee et al. 2015). Figure 13 however shows the studied reservoir in Field A is categorized as intermediate wet. The crossover point for the oil and water relative permeability curves is often indicative of the wettability. Where the crossover occurs with $Sw < 0.5$ we will assume an oil wet system. When crossover occurs with $Sw > 0.5$ this would normally be considered a water wet system. Cross over around 0.5 is generally considered as intermediate wettability.

Water saturation has an impact on wettability and consequently on residual oil saturation. Higher water saturation in a reservoir (e.g. intervals in the transition zone close to the FWL and OWC) promotes contact between grains and water and therefore increases the chance of the rock being water wet. On the contrary, lower water saturation facilitates the contact between the oil and grain surface and hence gives a greater potential for a wetting change from water wet toward oil wet (McPhee et al. 2015).

Finally, reservoir quality and particularly pore throat size and structures, control residual oil saturation (Sor) (Chatzis et al., 1983). Rocks with lower porosity, permeability, smaller and more heterogeneous pore throat sizes tend to show a higher Sor (Chatzis et al., 1983).

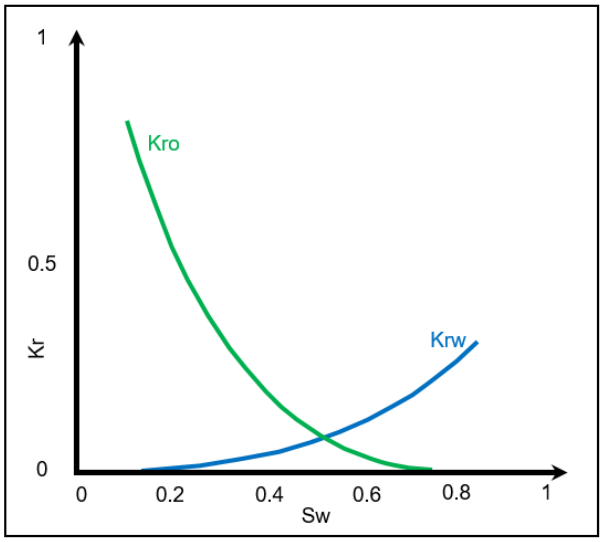

Figure 13: SCAL data shows intermediate wettability for the studied reservoir.

Figure 14 illustrates a frequency plot of residual oil saturation for different rock types from the fluid contact (FWL and OWC) to the base of the Sarvak (Mishrif) Fm in all studied wells. As shown in Figure 12 plots were calculated using open and cased hole logs.

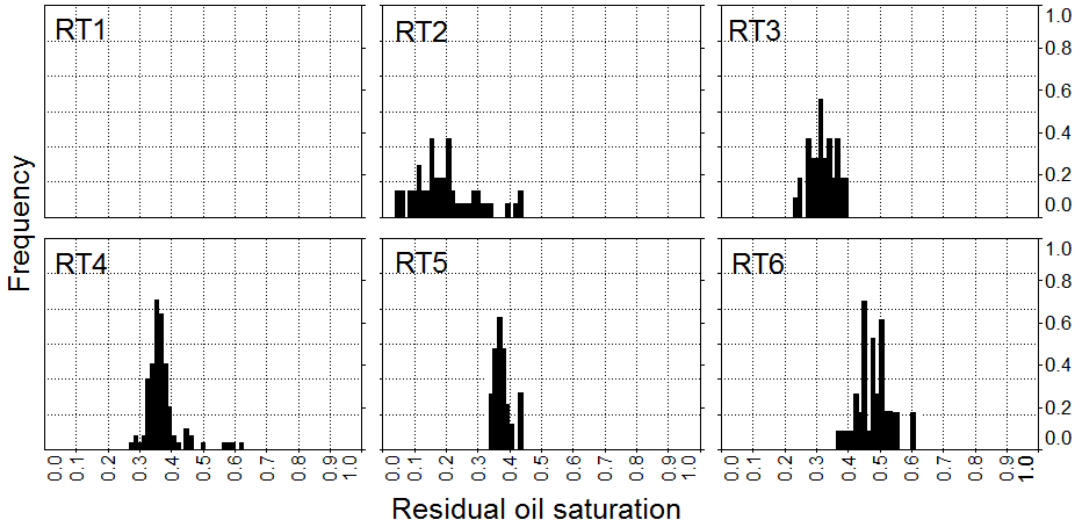

Figure 14: Frequency plot of residual oil saturation for different rock types for Sarvak (Mishrif) Formation below the FWL. These were calculated using open and cased hole logs.

The most important observations are:

- Residual oil below FWL and OWC occupies all rock types except for rock type 1.
- Rock type 6 presents maximum Sor below FWL and OWC.

The absence of residual oil below the FWL and OWC in rock type 1 was investigated by calculating and comparing the displacement and buoyancy pressures for each of the rock types. The pore throat size of pores occupied by residual oil reflects the level of capillary and gravitational force which act on the original oil. The Sarvak (Mishrif) Fm, initially contained water and was water-wet before oil migrated into the reservoir rock thereby displacing the water. To start oil migration into the reservoir, a displacement force was required to overcome the capillary forces holding the wetting fluid in place in the water saturated reservoir rock (Watts, 1987). This force was supplied by gravity operating upon the differential buoyancy of the two fluids resulting from their different densities (Watts, 1987). The displacement force or displacement pressure is equal in magnitude to the capillary pressure (Watts, 1987).

Therefore, the displacement pressure (Pc) of each rock type was calculated from the following equation:

$$P_c = \frac{2\sigma \cos\theta}{r} \qquad \text{Eq. (1)}$$

Where:

σ : hydrocarbon water interfacial tension

θ : contact angle

r: pore throat size in microns

The hydrocarbon water interfacial tension for the Sarvak (Mishrif) reservoir is about 0.03 N/M based on experimental data provided by field operator. The contact angle is zero as the reservoir was water wet before oil migration. Also, for each rock type, the representative pore throat size mode (Figure 9 and Table 2) was used as "r".

Buoyancy pressure (Pb) was calculated from the following equation:

$Pb = (\rho w - \rho o) * g * h$ Eq. (2)

Where:

Pb: buoyancy pressure

$(\rho w - \rho o)$: density difference between the water and oil, the density of formation water is 1.1 g/cc, and oil density is 0.85 g/cc.

g : gravity force (9.81 m/s2)

h : height above free water level, reservoir thickness is around 100 meters

Table 2: Pore throat size characteristics of each rock type. Note RT 6 has a bimodal pore system.

Rock type	Pore throat diameter (μm)		
	Minimum	Maximum	Mode
RT1	0.003	0.04	0.015
RT2	0.03	2.8	0.3
RT3	0.05	3	1
RT4	0.2	10.5	2.5
RT5	0.2	11	6
RT6	0.1	80	1.5 and 11

Table 3 illustrates the displacement force required to replace water by oil in each rock type during oil migration into the reservoir. The table also shows the buoyancy pressure calculated in the transition zone (minimum) and at the crest of the structure (maximum) which is independent of rock type. For rock type 1, the data show that for even the largest pore throats, the maximum available buoyancy pressure which is seen at the crest is insufficient to overcome the displacement pressure. Indeed, it is unlikely that oil migration into rock type 1 ever occurred and consequently no residual oil is seen at present day. In the other rock types, the buoyancy pressure has reached the pressure necessary for oil to enter the pores and displace water. All these rock types are therefore capable of having residual oil after a natural water flooding as a percentage of the oil would be trapped as isolated globules in the pores. Rock type 2 shows 10% to 40% Sor, rock types 3, 4 and 5 display 30 to 40% Sor and rock type 6 presents 45 to 55% Sor as calculated by wireline log data (Figure 12).

Table 3: Pore throat size, displacement pressure for each rock type and buoyancy pressure close to the fluid contact and at the crest. For oil migration into each rock type, buoyancy pressure should exceed displacement pressure.

Rock type	Pore throat size (micron)	Displacement pressure (Pa*1000)	Buoyancy in the transition zone (Pa*1000)	Buoyancy at the crest (Pa*1000)
1 (mode)	0.015	4000.0	25	550
1 (largest pore throat)	0.1	600.0	25	550
2	0.3	200.0	25	550
3	1	60.0	25	550
4	2.5	24.0	25	550
5	6	10.0	25	550
6 (small pore throat)	1.5	40.0	25	550
6 (large pore throat)	11	5.5	25	550

To investigate the presence of higher Sor in rock type 6 and assess the water flood process, the results of two water flood experiments on composite cores of rock type 6 and 4 in well A6 were used.

The first composite core was made up of four limestone rock pieces from rock type 6 of Upper Sarvak (Mishriff) Fm.. The composite core was 27.1 cm long and gave 405 mD as absolute permeability to water. The second composite core that contained two limestone pieces from rock type 4 of Upper Sarvak was 12.9 cm and gave 28 mD as absolute permeability to water. Details of these composite cores are shown in Table 4.

These tests were carried out under reservoir conditions using oil and water similar to the actual reservoir fluids. Details of these composite cores are shown in Table 4.

Table 4: Petrophysical details of selected composite cores for water flooding and results of water flooding.

Rock type	6	4
Core length (cm)	27.1	12.9
Air permeability (mD)	410	28
Water permeability (mD)	405	27
Porosity (%)	15.8	21.3
Initial water saturation (%)	13.6	17.3

Water injection was carried out at a constant rate of 10 cm^3/h which yielded a maximum differential pressure of 4.35 psi between the inlet and the outlet of both composite cores. Also, a sensibility to high injection rate was carried out using injection rate of 304 cm^3/h.

The following observations were made:

- **Composite core of rock type 4:** At an injection rate of 10 cm^3/h, water breakthrough occurred first at 31.1% pore volume (PV) of fluid injected. Prior to breakthrough, 27.4% Initial Oil in Place (IOIP) had been recovered. An additional 26% IOIP was recovered after

water breakthrough leading to the final oil recovery of 53.4% of IOIP. At the end of the 10 cm3/h water injection process, Sor was calculated at 38.5% (Table 5 and Figure 13).

- **Composite core of rock type 6:** At an injection rate of 10 cm^3/h, water breakthrough occurred first at 15% PV of fluid injected. Prior to this, 16% of IOIP had been recovered. An additional 5.5% of IOIP was recovered after water breakthrough leading to the final oil recovery of 21.7% of IOIP. At the end of 10 cm3/h water injection process, Sor and Sw were calculated to be 67.6 % and 32% respectively (Table 5 and Figure 15).

Like the Sor calculated by logs (Figure 14), the composite core of rock type 6 with higher permeability and lower Swi (Table 1) shows higher Sor which is indication of an earlier breakthrough compared to the composite core of rock type 4.

Table 5: Petrophysical details of selected composite cores for water flooding and results of water flooding test.

Composite core		Composite core of rock type 4	Composite core of rock type 6
Reservoir quality	Porosity (%)	20	17
	Air permeability (mD)	28	410
	Water permeability (mD)	27	405
	Permeability to reservoir oil at Swi (mD)	26	398
	Irreducible water saturation (Swi)	13.6	17.3
Test	Initial injection rate (cm3/h)	10	10
	Front advance velocity (m/day)	0.34	0.81
Water breakthrough	Pore volume (PV) injected	31.1	16.2
	Cumulative oil recovery (% IOIP)	27.4	16.2
End of water flood at 10 cm^3/h	Pore volume (PV) injected	537.7	432
	Ultimate oil recovery (% IOIP)	53.4	21.7
	Sor (%)	38.5	67.6

Pore throat size and its distribution are the main factors that control reservoir quality (Johnson, 1998). Higher Sor in rock type 6 was attributed to its bimodal pore throat diameter distribution.

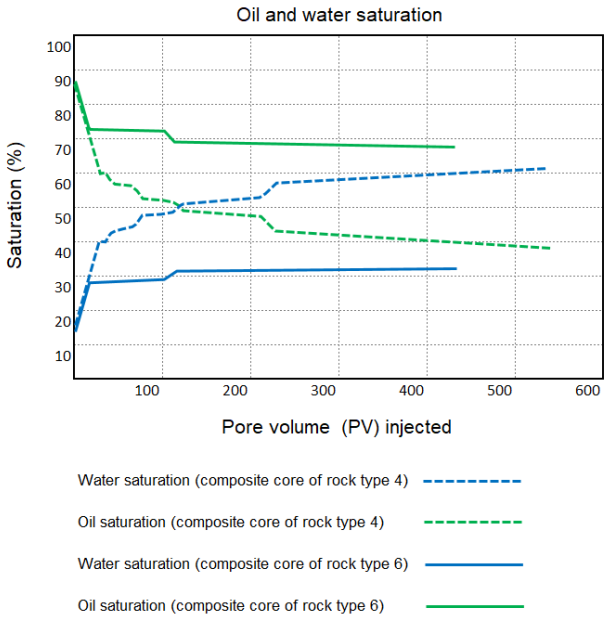

Figure 15: Oil and water saturation in composite cores of rock type 4 and 6 at 10 cm^3/h

In rock type 6, water typically follows a preferential flow path through the larger mode of pore throat size distribution, where the pore throat diameter exceeds 10-15 microns and consequently some oil is by-passed (Figure 16).

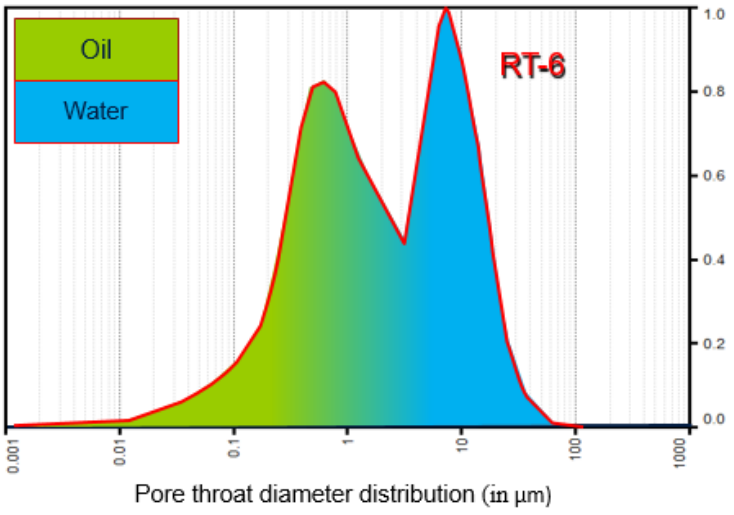

Figure 16: Pore throat diameter distribution of rock type 6 in µm. In this rock type water follows a preferential flow path through the larger mode of pore throat size distribution and some oil is by-passed in smaller pores

In contrast, the narrow and well sorted pore throat size distribution in rock type 4 (Figure 17) connected all the pores with injected water at the low rate of injection (10 cm^3/h) and therefore strongly increased the oil recovery leading to less residual oil compared to rock type 6. This hypothesis is strengthened by the small additional recovery in rock type 4 (15.8 % lOIP) when implementing a high injection rate (304 cm^3/h): this rate led to the sweep of a few additional small pores and yielded a cumulative final oil recovery of 69.2 °/o IOIP (Table 6).

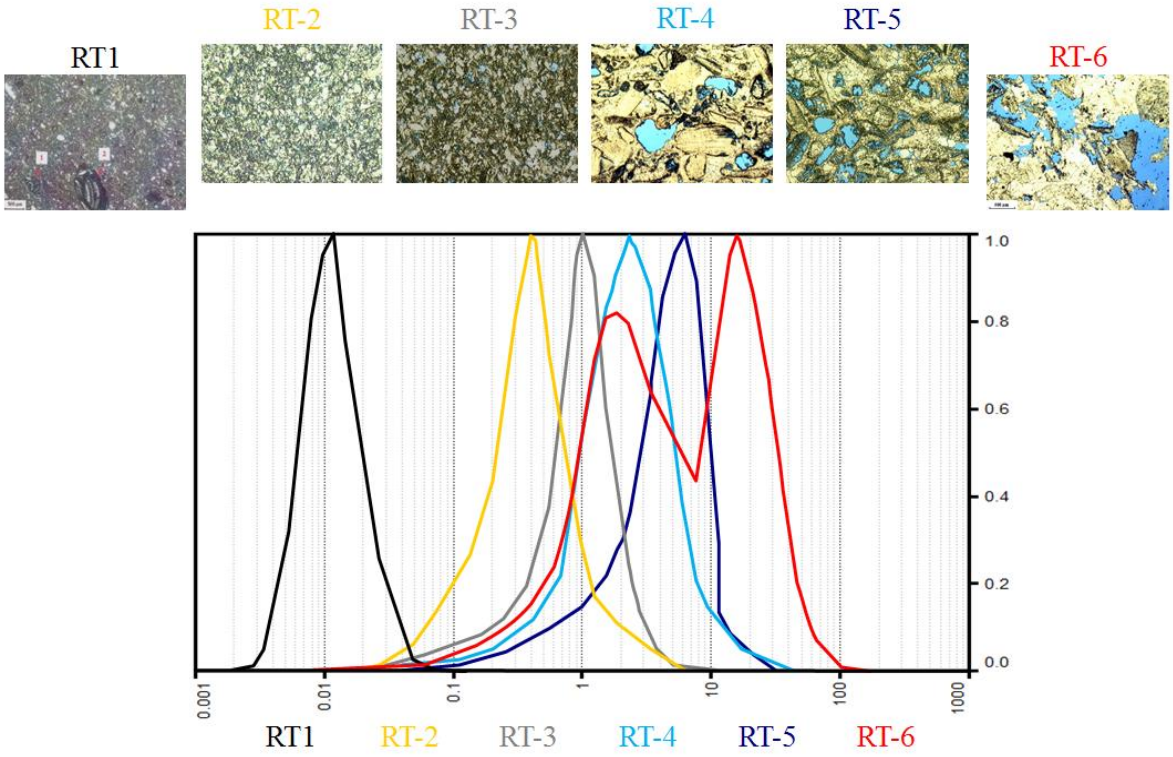

Figure 17: Pore throat diameter distribution of each rock type (in µm).

According to the fluid density, gravity forces through segregation are lower than viscous forces in any case. Therefore, in the lab experiment at reservoir conditions, the recovery mechanism is mainly driven by viscous forces and controlled by capillary forces. Capillary forces significantly prevent oil from being expelled at a low rate. A higher injection rate did not recover more additional oil in rock type 6.

Table 4: Results of water flooding test at 304 cm^3/h shows less residual oil and higher recovery factor in well sorted pore throat size distribution in rock type 4.

End of water flood at 304 cm^3/h	Injection rate (cm^3/h)	304
	Front advance velocity (m/day)	8.02
	PV injected (%)	2628.6
	Ultimate oil recovery (% IOIP)	69.2
	Sor (%)	25.5

7. Conclusions

In this case study, six major rock types were classified in cored wells. Rock types were identified based on data integration, with reservoir quality increasing from rock type 1 to 6. Each rock type presents a unique pore throat size distribution and FZI which illustrate their different reservoir behaviour.

Rock type 1 is was deposited in the protected platform and mainly comprises wackstone with peloids and frequent forams. Rock type 2 is was deposited within the upper slope. It is composed of wackstone and packstone with benthic forams. Rock type 3 is the main rock type of the lower slope and is largely composed of packstone. Rock types 4, 5 and 6 were deposited in a shoal environment. Cementation decreases from rock type 4 to 6 while permeability, pore throat size and FZI increase from rock type 4 to 6.

The amount of residual oil in each rock type was defined from the fluid contact to the base of the reservoir and the following observations were made:

- Residual oil is found in all rock types except for rock type 1.
- Maximum Sor is seen in rock type 6.

The absence of residual oil in rock type 1 was related to its very high displacement pressure and consequently it is unlikely that oil migration into rock type 1 ever occurred.

Maximum Sor is seen in rock type 6 because of its bimodal pore throat size distribution. In this rock type, only pores with larger pore throat diameters (pore throat diameter exceeds 10-15 microns) have been water flooded. This occurs because water typically follows a preferential flow path through the high permeability zones with larger pore throat diameter and consequently some oil is by-passed in pores with smaller pore throat size.

The results of this study may be used as a guideline in production scenarios and enhanced oil recovery (EOR) projects. It is suggested that residual oil saturations below fluid contact are used as a guide to determine the final residual oil saturation in the transition zone after production and water flooding. Also, the results of this study revealed residual oil saturation varies depending on pore throat size distribution. Maximum residual oil saturation is seen when pore throat size distribution is bio-modal.

Acknowledgments

The authors would like to gratefully acknowledge and appreciate the support of Aberdeen Formation Evaluation Society (AFES) and Baker Hughes for their sponsorship and Emerson for providing Geolog software for development of this study.

REFERENCES

ALABI, G., KASTEN, R., CHITAL, V., YADAVALLI, S., PICCOLI, L., 2014. Value of petrophysical measurements at various scales- a lacustrine carbonate example from Campos Basin, Brazil. SPWLA 55th Annual Logging Symposium, May 2014, Abu Dhabi.

ALEIDAN, A., KWAK, H., MULLER, H., and ZHOU, X., 2017. Residual-Oil Zone: Paleo-Oil Characterization and Fundamental Analysis. Society of Petroleum Engineers, 260-268.

ALIAKBARDOUST, E., RAHIMPOUR-BONAB, H., 2013. Effects of pore geometry and rock properties on water saturation of a carbonate reservoir, Journal of Petroleum Science and Engineering, 112, 296-309.

Al-FARISI, O., BELGAIED, A., ELHAMI, M., KADADA,T., AL-JEFRI, G. and BARKAWI, A., 2004. Electrical Resistivity and Gamma Ray Logs: Two Physics for Two Permeability Estimation Approaches in Abu Dhabi Carbonates, SPE 88687, presented at the 11th SPE Abu Dhabi International Petroleum Exhibition and Conference, Abu Dhabi, U.A.E., October. 10-13.

Al-HABSHI, A., DARWISH, D.A., HAMDY, T. and SHEBL, H., 2003. Application of Sequence Stratigraphy and Petrography in Preparation of Reservoir Rock Typing Scheme in One of Thamama Gas Reservoirs of Onshore Abu Dhabi, SPE 81533, presented at the 13th SPE Middle East Oil Show & Conference, Bahrain, June 9-12.

ALI-NANDAL, J. and GUNTER, G., 2003. Characterizing Reservoir Performance for the Mahogany 20 Gas Sand Based on Petrophysical and Rock Typing Methods, SPE 81048, presented at the SPE Latin American and Caribbean Petroleum Engineering Conference, Port-of-Spain, Trinidad, West Indies, April. 27-30.

ALSHARHAN, A.S. and NAIRN, A.E.M., 1997. Sedimentary Basins and Petroleum Geology of the Middle East. Elsevier science publication, Netherland.

AMAEFULE, J.O., ALTUNBAY, M., TIAB, D., KERSEY, D.G. and KEELAN, D.K., 1993. Enhanced reservoir description: using core and log data to identify hydraulic (flow) units and predict permeability in uncored intervals/wells. SPE 26436.

ARCHIE, G.E., 1950. Introduction to Petrophysics of reservoir rocks, AAPG Bulletin V.34, P. 943-961.

BOADA, E., 2001. Rock Typing: Key Approach for Maximizing Use of Old Well Log Data in Mature Fields, Santa Rosa Field, Case Study," SPE 69459, presented at the SPE Latin American and Caribbean Petroleum Engineering Conference, Buenos Aires, Argentina, March 25-29.

CHANDRA, V.., BARNETT, A., CORBETT, P., GEIGER, S., WRIGHT, P., STEELE, R., and MILROY, P., 2015. Effective integration of reservoir rock-typing and simulation using near-wellbore upscaling. Journal of Marine and Petroleum Geology, 67, 307-326.

CHITALE, V., ALABI, G., GRAMIN, P., LEPLEY, S. and PICCOLI, L., 2015. Reservoir Characterization challenges due to multiscale spatial heterogeneity in the PreSalt carbonate Sag Formation, North Campos Basin, Brazil: PETROPHYSICS, V56, No.6, 552-576.

CHATZIS, I., MORROW, N. R., and LIM, H. T., 1983. Magnitude and Detailed Structure of Residual Oil Saturation. Society of Petroleum Engineers. doi:10.2118/10681-PA

DAVIES, K.K., WILLIAMS, B.P.J., and VESSELL, R.K., 1991. Reservoir Geometry and Internal Permeability Distribution in Fluvial, Tight Gas Sandstones, Travis Peak Formation, Texas, SPE 21850, presented at the Rocky Mountain Regional Meeting and Low-Permeability Reservoirs Symposium, Denver, April 15-17.

DUNHAM, R. J., 1962. Classification of carbonate rocks according to depositional texture. In: Ham, W. E. (ed.), Classification of carbonate rocks: American Association of Petroleum Geologists Memoir, p. 108-121.

FARZADI, P., 2006. The development of Middle Cretaceous carbonate platforms, Persian Gulf, Iran: Constraints from seismic stratigraphy, well and biostratigraphy. Petroleum Geoscience, 12, 59-68.

GHADAMI. N., RASAEI, M.R., HEJRI, SH., SAJEDIAN, A., AFSARI, KH., 2015. Consistent porosity-permeability modeling, reservoir rock typing and Hydraulic flow

unitization in a giant carbonate reservoir, Journal of Petroleum Science and Engineering, 131, 58-69.

GOMES, J.S., RIBEIRO, M.T., STROHMENGER, C.J., NEGAHBAN, S. and KALAM, M.Z., 2008. Carbonate reservoir rock typing-The link between geology and SCAL, SPE, 118284.

HAROUAKA, A., TRENTHAM, B., and MELZER, S., 2013. Long Overlooked Residual Oil Zones (ROZs) Are Brought into the Limelight. Society of Petroleum Engineers, 167209.

HARTMANN, D.J and BEAUMONT, E.A., 2000. Predicting reservoir system quality and performance. AAPG, 2000.

HEYDARI-FARSANI, E., Neilson, J. E., Alsop, G. I., Hamidi, H., 2019. Tectonic controls on residual oil saturation below the present-day fluid contact level in reservoirs of the Persian Gulf, Journal of Asian Earth Sciences, 104133, ISSN 1367-9120,

JOHNSON, R.W., 1998. The Handbook of Fluid Dynamics, Crc Press.

HONARPOUR, M. M., NAGARAJAN, N. R., GRIJALBA CUENCA, A., VALLE, M. and ADESOYE, K., 2010. Rock-Fluid Characterization for Miscible CO2 Injection: Residual Oil Zone, Seminole Field, Permian Basin. SPE 133089.

JORDAN, C.F., CONNALLY, T.C. and VEST, H.A., 1985. Middle Cretaceous carbonates of the Mishrif Formation, Fateh Field, Offshore Dubai, U.A.E., In Roehl, P.O. & Coquette, P.W. (eds) Carbonate Petroleum Reservoirs. Springer-Verlag, New York, 425-442.

KIRKHAM, A., BIN JOMA, M., MCKEAN, T. A. M., PALMER, A. F., SMITH, M. J., THOMAS, H., and TWOMBLEY, B., 1996. Fluid saturation prediction in a transition zone. GeoArabia 1(4), 551-566.

KOPERNA, G. J., MELZER, L. S., and KUUSKRAA, V. A., 2006. Recovery of Oil Resources from the Residual and Transitional Oil Zones of the Permian Basin. SPE 102972, Presented at the SPE annual technical conference and exhibition, San Antonio, TX, September 24-27

LEE, S.H., KHARGHORIA, A. and DATTA-GUPTA, A., 2002. Electrofacies Characterization and Permeability Predictions in Complex Reservoirs, SPE 78862, presented at SPE Reservoir Evaluation & Engineering, 237-248.

MARQUEZ, L.J., GONZALEZ, M., GAMLE, S., 2001. Improved Reservoir Characterization of a Mature Field Through an Integrated Multi-Disciplinary Approach: LL-04 Reservoir, Tia Juana Field, Venezuela, SPE 71355, presented at the SPE Annual Technical Conference and Exhibition, New Orleans, LA, 30 September–3 October.

MCPHEE, C., REED, J., ZUBIZARRETA, I., 2015. Core Analysis: A Best Practice Guide, Elsevier, Development in Petroleum Science, Volume 64.

MEZLER, S., KOPERNA, G., and KUUSKRAA, V., 2006. The origin and resource potential of residual oil zones, SPE 102964, Presented at the SPE annual technical conference and exhibition, San Antonio, TX, September 24-27.

NOURI-TALEGHANI, M., KADKHODAIE, A. And KARIMI, K., 2015. Determining hydraulic flow units using a hybrid neural network and multi-resolution graph-based clustering method: Case study from Ssouth Ppars gasfield, Iran, Journal of Petroleum Geology Vol. 38, no. 1, January.

OHEN, H.A., ERIAN, A., ALI, L., GUZMAN, D., GUERRERO, O., OCHOA, J. and VALDIVIESO, L., 2004. Integrated Reservoir Study of Shushufindi Field - Dynamic Modeling, SPE 89465, presented at the SPE/DOE Fourteenth Symposium on Improved Oil Recovery, Tulsa, OK, April 17-21.

O'SULLIVAN, T., PRAVEER, K., SHANLEY, K., DOLSON, J.C., WOODHOUSE, R., 2010. Residual hydrocarbons—a trap for the unwary, SPE 128013.

PARKER, A. R., and RUDD, J. M., 2000. Understanding and Modeling Water Free Production in Transition Zones: A Case Study. SPE 59412.

PELISSIER, J., HEDAYATI, A. A., ABGRALL, E., and PLIQUE, J., 1980. Study of Hydrodynamic Activity in the Mishrif Fields, Offshore Iran. Society of Petroleum Engineers. doi:10.2118/7508-PA.

PEREZ, H.H., DATTA-GUPTA, A., and MISHRA, S., 2003. The Role of Electrofacies, Lithofacies, and Hydraulic Flow Units in Permeability Predictions from Well Logs: A Comparative Analysis Using Classification Trees, SPE 84301, presented at the SPE Annual Conference and Exhibition, Denver, CO, October 5-8.

PEREZ, H.H., DATTA-GUPTA, A. and MISHRA, S., 2005. The role of electrofacies, lithofacies, and hydraulic flow units in permeability prediction from well logs: a comparative analysis using classification trees. SPE, 84301, 143-155.

PORRAS, J.C. and CAMPOS, O., 2001. Rock Typing: A Key Approach for Petrophysical Characterization and Definition of Flow Units, Santa Barbara Field, Eastern Venezuela Basin, SPE 69458 presented at the SPE Latin American and Caribbean Petroleum Engineering Conference, Buenos Aires, Argentina, March 25-28.

PORRAS, J.C., BARBATO, R., and KHAZEN, L., 1999. Reservoir Flow Units: A Comparison Between Three Different Models in the Santa Barbara and Pirital Fields, North Monagas Area, Eastern Venezuela Basin, SPE, 53671 presented at the SPE Latin American and Caribbean Petroleum Engineering Conference, Caracas, Venezuela, April 21-23.

SHENAWI, S., WHITE, J., ELRAFIE, E. and ELKILANI, K., 2007, Permeability and Water Saturation Distribution by Lithologic Facies and Hydraulic Units: A Reservoir Simulation Study, SPE 105273, presented at the 15th SPE Middle East Oil & Gas Show and Conference, Kingdom of Bahrain, March 11-14.

SLATT, R.M., 2007, Stratigraphic Reservoir Characterization for Petroleum Geologists, Geophysicists, and Engineers, Elsevier Publication.

SOTO, B, 2001. Improved Reservoir Permeability Models from Flow Units and Soft Computing Techniques: A Case Study, Suria and Reforma-Libertad Fields, Columbia, SPE 69625, presented at the SPE Latin American and Caribbean Petroleum Engineering Conference, Buenos Aires, Argentina, March. 25-28.

THOMASEN, J. B., and JACOBSEN, N. L., 1994. Dipping Fluid Contacts in the Kraka Field, Danish North Sea. Society of Petroleum Engineers. doi:10.2118/28435-MS.

VARAVUR, S., SHEBL, H., SALMAN, S.M., DABBOUK, C., 2005. Reservoir Rock Typing in a Giant Carbonate, SPE 93477, presented at the 14th SPE Middle East Oil and Gas show and Conference held in Bahrain, March 12-15.

VEJBAEK, O. V., FRYKMAN, P., and NIELSEN, C. M., 2005. The history of the hydrocarbon filling of Danish chalk fields. Geological Society of London 6, 1331-1345.

Watts, N. L., 1987, Theoretical aspects of cap-rock and fault seals for single and two-phase hydrocarbon columns, Marine and Petrol. Geol., v. 4, p. 274-307.

ZIEGLER, M.A., 2001. Late Permian to Holocene paleofacies evolution of the Arabian Plate and its hydrocarbon occurrences. GeoArabia 6, 445–504.